Engineering the refractive index of three-dimensional photonic crystals through multilayer deposition of CdS films

Dario Buso[1,2*], Elisa Nicoletti[1], Jiafang Li[1], and Min Gu[1]

[1]Centre for Micro-Photonics and CUDOS
Faculty of Engineering and Industrial Sciences - Swinburne University of Technology
Hawthorn, VIC 3122 (Australia)
[2]CSIRO – Material Science and Engineering
Clayton South MDC, VIC 3169 (Australia)
**dario.buso@csiro.au*

Abstract: Woodpile photonic crystals are amongst the preferred candidates for the next generation of photonics components. However, the photocurable resists used to produce them still lack the optical properties (high-n, non-linearity) suitable for photonics applications. A chemical bath deposition protocol has been adapted to deposit high-*n*/non-linear chalcogenide CdS on the surface of Ormocer® woodpiles. The deposition parameters have been adjusted to obtain heterogeneous growth of CdS layers on the Ormocer® surface. The layers shift the photonic band-gap and increase its amplitude by more than 15%. Software simulation confirmed that the woodpile effective refractive index underwent an excess of 30% increase.

OCIS codes: (230.5298) Photonic Crystals; (160.6000) Semiconductor Materials; CdS

References and Links

1. P. Russell, "Photonic band cap guidance in optical fibers," Science **299**, 358 (2003).
2. S. Noda, "Applied physics. Seeking the ultimate nanolaser," Science **314**(5797), 260–261 (2006).
3. L. F. Mollenauer, "Physics. Nonlinear optics in fibers," Science **302**(5647), 996–997 (2003).
4. A. D. Greentree, C. Tahan, J. H. Cole, and L. C. L. Hollenberg, "Photonic band cap guidance in optical fibers," Nat. Phys. **2**, 856 (2006).
5. E. Yablonovitch, "Inhibited spontaneous emission in solid-state physics and electronics," Phys. Rev. Lett. **58**(20), 2059–2062 (1987).
6. S. John, "Strong localization of photons in certain disordered dielectric superlattices," Phys. Rev. Lett. **58**(23), 2486–2489 (1987).
7. S. Y. Lin, J. G. Fleming, D. L. Heterington, B. K. Smith, R. Biswas, K. M. Ho, M. M. Sigalas, W. Zubrzycki, S. R. Kurtz, and J. Bur, "A three-dimensional photonic crystal operating at infrared wavelengths," Nature **394**(6690), 251–253 (1998).
8. S. Noda, K. Tomoda, N. Yamamoto, and A. Chutinan, "Full three-dimensional photonic bandgap crystals at near-infrared wavelengths," Science **289**(5479), 604–606 (2000).
9. B. T. Holland, C. F. Blanford, and A. Stein, "Synthesis of macroporous minerals with highly ordered three-dimensional arrays of spheroidal voids," Science **281**(5376), 538–540 (1998).
10. J. E. G. J. Wijnhoven, and W. L. Vos, "Preparation of photonic crystals made of air spheres in titania," Science **281**(5378), 802–804 (1998).
11. A. Blanco, E. Chomski, S. Grabtchak, M. Ibisate, S. John, S. W. Leonard, C. Lopez, F. Meseguer, H. Miguez, J. P. Mondia, G. A. Ozin, O. Toader, and H. M. van Driel, "Large-scale synthesis of a silicon photonic crystal with a complete three-dimensional bandgap near 1.5 micrometres," Nature **405**, 437-440 (2000).
12. M. Campbell, D. N. Sharp, M. T. Harrison, R. G. Denning, and A. J. Turberfield, "Fabrication of photonic crystals for the visible spectrum by holographic lithography," Nature **404**, 53-56 (1999).
13. P. V. Braun, S. A. Rinne, and F. García-Santamaria, "Introducing Defects in 3D Photonic Crystals: State of th Art," Adv. Mater. **18**(20), 2665–2678 (2006).
14. S. A. Rinne, F. García-Santamaria, and P. V. Braun, "Embedded cavities and waveguides in three-dimensional silicon photonic crystals," Nat. Photonics **2**(1), 52–56 (2008).
15. B. H. Cumpston, S. P. Ananthavel, S. Barlow, D. L. Dyer, J. E. Ehrlich, L. L. Erksine, A. A. Heikal, S. M. Kuebler, I. Y. S. Lee, D. McCord-Maughon, J. Qin, H. Röckel, M. Rumi, X. L. Wu, S. L. Marder, and J. W.

#119435 - $15.00 USD Received 3 Nov 2009; revised 17 Dec 2009; accepted 18 Dec 2009; published 7 Jan 2010

Perry, "Two-photon polymerization initiators for three-dimensional optical data storage and microfabrication," Nature **398**(6722), 51–54 (1999).
16. M. Straub, and M. Gu, "Near-infrared photonic crystals with higher-order bandgaps generated by two-photon photopolymerization," Opt. Lett. **27**(20), 1824–1826 (2002).
17. M. Deubel, G. von Freymann, M. Wegener, S. Pereira, K. Busch, and C. M. Soukoulis, "Direct laser writing of three-dimensional photonic-crystal templates for telecommunications," Nat. Mater. **3**(7), 444–447 (2004).
18. Y. Jun, P. Nagpal, and D. J. Norris, "Thermally Stable Organic-Inorganic Hybrid Photoresists for Fabrication of Photonic Band Gap Structures with Direct Laser Writing," Adv. Mater. **20**(3), 606–610 (2008).
19. J. Serbin, A. Ovsianikov, and B. Chichkov, "Fabrication of woodpile structures by two-photon polymerization and investigation of their optical properties," Opt. Express **12**(21), 5221–5228 (2004).
20. B. Jia, S. Wu, J. Li, and M. Gu, "Near-infrared high refractive-index three-dimensional inverse woodpile photonic crystals generated by a sol-gel process," J. Appl. Phys. **102**(9), 096102 (2007).
21. S. Wong, M. Deubel, F. P. Willard, S. John, G. A. Ozin, M. Wegener, and G. Von Freymann, "Direct Laser Writing of Three-Dimensional Photonic Crystals with a Complete Photonic Bandgap in Chalcogenide Glasses," Adv. Mater. **18**(3), 265–269 (2006).
22. E. Nicoletti, G. Zhou, B. Jia, M. J. Ventura, D. Bulla, B. Luther-Davies, and M. Gu, "Observation of multiple higher-order stopgaps from three-dimensional chalcogenide glass photonic crystals," Opt. Lett. **33**(20), 2311–2313 (2008).
23. J. Serbin, and M. Gu, "Experimental evidence for superprism effects in three-dimensional polymer photonic crystals," Adv. Mater. **18**(2), 221–224 (2006).
24. J. Li, B. Jia, and M. Gu, "Engineering stop gaps of inorganic-organic polymeric 3D woodpile photonic crystals with post-thermal treatment," Opt. Express **16**(24), 20073–20080 (2008).
25. R. Xie, T. Sekiguchi, D. Li, D. Yang, and M. Jiang, "Precise fabrication of point defects in self-assembled three-dimensional macroporous photonic crystals," J. Phys. Chem. B **110**(3), 1107–1110 (2006).
26. Y. C. Lee, T. J. Kuo, C. J. Hsu, Y. W. Su, and C. C. Chen, "Fabrication of 3D Macroporous Structures of II-VI and III-V Semiconductors Using Electrochemical Deposition," Langmuir **18**(25), 9942–9946 (2002).
27. Y. R. Lin, C. Y. Kuo, and S. Y. Lu, "Stop band tuning of three-dimensional photonic crystals through coating of semiconductor materials," Appl. Phys., A Mater. Sci. Process. **79**(7), 1741 (2004).
28. Y. A. Vlasov, V. N. Astratov, O. Z. Karimov, A. A. Kaplyanskii, V. N. Bogomolov, and A. V. Prokofiev, "Existence of a photonic pseudogap for visible light in synthetic opals," Phys. Rev. B **55**(20), 357 (1997).
29. Z. Lei, J. Li, Y. Ke, Y. Zhang, H. Wang, and G. He, "fabrication of macroporous cadmium sulfide with three-dimensional structure by solvothermal synthesis," J. Mater. Chem. **11**(7), 1778–1780 (2001).
30. L. K. Teh, V. Furin, A. Martucci, M. Guglielmi, C. C. Wong, and F. Romanato, "Electrodeposition of CdSe on nanopatterned pillar arrays for photonic and photovoltaic applications," Thin Solid Films **515**(15), 5787–5791 (2007).
31. L. M. Chuang, H. K. Fu, and Y. F. Chen, "Fabrication and optical properties of two-dimensional photonic crystals of CdSe pillars," Appl. Phys. Lett. **86**(6), 061902 (2005).
32. Z. B. Sun, X. Z. Dong, W. Q. Chen, S. Nakanishi, X. M. Duan, and S. Kawata, "Multicolor Polymer Nanocomposites: In Situ Synthesis and Fabrication of 3D Microstructures," Adv. Mater. **20**(5), 914–919 (2008).
33. J. M. Doña, and J. Herrero, "Chemical bath deposition of CdS thin films: An approach to the chemical mechanism through Study of the film microstructure," J. Electrochem. Soc. **144**(11), 4081 (1997).
34. D. Buso, L. Palmer, V. Bello, G. Mattei, M. Post, P. Mulvaney, and A. Martucci, "Self-assembled gold nanoparticle monolayers in sol-gel matrices: synthesis and gas sensing applications," J. Mater. Chem. **19**(14), 2051 (2009).
35. H. Metin, and R. Esen, "Annealing studies on CBD grown US thin films," J. Cryst. Growth **258**(1-2), 141–148 (2003).
36. R. Swanepoel, "Determination of the thickness and optical constants of amorphous silicon," J. Phys. E Sci. Instrum. **16**(12), 1214 (1983).
37. M. Kar, and B. S. Verma, "Improvements in the determination of extinction coefficients of a thin film using an envelope method," J. Opt. A, Pure Appl. Opt. **7**(10), 599–603 (2005).
38. E. Çetinörgü, C. Gümüş, and R. Esen, "Effects of deposition time and temperature on the optical properties of air-annealed chemical bath deposited CdS films," Thin Solid Films **515**(4), 1688–1693 (2006).
39. M. D. Archbold, D. P. Halliday, K. Durose, T. P. A. Hase, D. S. Boyle, S. Mazzamuto, N. Romeo, and A. Bosio, "Development of low temperature approaches to device quality CdS: a modified geometry for solution growth of thin films and their characterisation," Thin Solid Films **515**(5), 2954–2957 (2007).
40. MPB software package, http://ab-initio.mit.edu/wiki/index.php/MIT_Photonic_Bands.
41. J. Serbin, and M. Gu, "Superprism phenomena in polymeric woodpile structures," J. Appl. Phys. **98**(12), 123101 (2005).
42. J. Serbin, A. Egbert, A. Ostendorf, B. N. Chichkov, R. Houbertz, G. Domann, J. Schulz, C. Cronauer, L. Fröhlich, and M. Popall, "Femtosecond laser-induced two-photon polymerization of inorganic-organic hybrid materials for applications in photonics," Opt. Lett. **28**(5), 301–303 (2003).
43. J. Li, B. Jia, G. Zhou, C. Bullen, J. Serbin, and M. Gu, "Spectral Redistribution in Spontaneous Emission from Quantum-Dot Infiltrated 3D Woodpile Photonic Crystals for Telecommunications," Adv. Mater. **19**(20), 3276–3280 (2007).

#119435 - $15.00 USD Received 3 Nov 2009; revised 17 Dec 2009; accepted 18 Dec 2009; published 7 Jan 2010

44. J. Li, B. Jia, G. Zhou, and M. Gu, "Fabrication of three-dimensional woodpile photonic crystals in a PbSe quantum dot composite material," Opt. Express **14**(22), 10740–10745 (2006).
45. R. S. Mane, and C. D. Lokhande, "Chemical deposition method for metal chalcogenide thin films," Mater. Chem. Phys. **65**(1), 1–31 (2000).
46. L. Zhou, D. S. Boyle, K. Govender, and P. O'Brien, "High efficiency solution infiltration routes to thin films with photonic properties," J. Exp. Nanosci. **1**(2), 221–233 (2006).
47. M. Maldovan, E. L. Thomas, and C. W. Carter, "Layer-by-layer diamond like woodpile structure with a large photonic band gap," Appl. Phys. Lett. **84**(3), 362–364 (2004).

1. Introduction

Artificial micro-structures with an optical band-gap equivalent to the energy-gap in semiconductors promise a generation of new devices addressing the demand for ever-faster computers and optical communications [1–4]. Named photonic crystals (PhCs), these structures represent a new class of devices for guiding and processing light through the spatial periodicity of their dielectric function. Matter-light interaction is obtained when such periodicity matches the wavelength range of the electromagnetic field to manipulate. The fabrication of convincing tridimensional modular arrangements using high refractive index (*n*) solids have been the main goal of researchers since the publication of the conceptual base for 3D PhCs and photonic band gap (PBG) materials, back in 1987 [5,6].

The successful realization of high-quality PBG materials is determined by two key factors: firstly, the ability to build 3D arrays through refined micro-fabrication techniques and secondly, the need for control and improvement of the materials optical properties (high-*n*, optical *non-linearity* etc). Regarding the first point, a variety of fabrication methods have been developed to produce photonic structures, ranging from conventional lithography [7,8], colloidal self-assembly [9–11] (SA) and holographic lithography (HL) [12]. Although very effective in producing PBG materials, these approaches (especially SA and HL) still require complex and external multi-step procedures to introduce intentional geometric defects inside the micro-structures [13,14]. In this sense, the alternative represented by the direct laser writing (DLW) approach is effective, flexible and straightforward to realize arbitrary-shaped photonic structures in three dimensions [15,16]. Amongst DLW techniques, two-photon polymerization (TPP) offers the most promise for creating complex three-dimensional structures at fine length scales (tens of nanometers). In the TPP technique, the focus of a laser beam is translated within a photo-polymerizable matrix, which is locally cross-linked through the excitation of a two-photon initiator. The possibility to obtain photonic structures with TPP has been extensively demonstrated [15,16], and in particular PhCs in form of woodpile assemblies have been addressed as the most promising [16,17]. However, the majority of such structures have been fabricated using conventional organic or hybrid organic/inorganic photo-resists of low refractive index. As a consequence, their low *n* and low optical non-linearity make them unfit to provide the 3D structure with strong PBG confinement and versatile PBG engineering, both of which are pursued for device applications [17,18]. Attempts to obtain high-*n* woodpile PhCs have been made using the resist structures as a template for high-*n* semiconductors infiltration [19,20], or even, and more convincingly, using DLW directly on high-*n* photo-sensitive inorganic chalcogenides [21,22]. The limitation of the infiltration approach lies in the complicated procedures, expensive facilities and strict requirement on the mechanical stability of the template. Therefore, it is difficult to scale down the structural elements to achieve PBG below 2 μm. On the other hand, the DLW of chalcogenide glass still presents unresolved issues related to spherical aberration and depth-dependent intensity decrease of the laser focus spot when writing such high-*n* materials. However, what reported by Wong et al. [21] is remarkably the first example of complete PBG measured in a woodpile structure obtained by DLW ever reported.

In this work a fast protocol to precisely engineer the effective *n* value of a hybrid organic/inorganic template woodpile structure is described, and the effect on the PBG over a wide range of wavelengths in the telecommunications regime is reported. High-*n* and non-

#119435 - $15.00 USD Received 3 Nov 2009; revised 17 Dec 2009; accepted 18 Dec 2009; published 7 Jan 2010

linear CdS multilayered films have been deposited on the surface of a 3D PhC fabricated with TPP technique using a modified chemical bath deposition (CBD) approach [33,45,46]. The protocol has been optimized for the controlled deposition of a binary chalcogenide on the whole surface of a 3D PhC template. The method has the inherent advantage of creating a homogenous coating on the woodpile structure along all spatial directions, therefore bypassing a crucial limitation typical of mono-directional coating techniques. The coating can be performed at room conditions and it is extremely inexpensive; it works at moderate temperature with no need of controlled atmosphere and/or high-vacuum systems [34]. Furthermore, the possibility to perform the protocol on non-conductive substrates (Ormocer® is an organic-inorganic hybrid) gives further advantage compared to electro-chemical techniques [31]. The overall protocol is cheap, fast and highly reproducible.

2. Experimental details

The micron-scale PhC was fabricated using a designed Ormocer® (OrmoCore B59, 1.8% Irgacure 369) from MicroResist Technology. Femtosecond laser pulses (~200fs) operating at 580nm were focused into the resist with an oil immersion objective (Olympus, numerical aperture 1.4, 100 ×) using a 76MHz repetition rate according to [43]. The polymerized PhC was developed using a 1:1 v/v mixture of 2,4-pentanedione and 2-propanol.

Prior to CdS deposition, the PhC surface was pre-sylanized with immersion in a 5% (wt) aminopropyl triethoxy silane (APTES) solution in toluene, at 60°C for 5 minutes. CdS was deposited using a modified chemical bath deposition (CBD) approach. A solution of cadmium acetate (0.33 g), ammonium acetate (0.06 g) and ammonium hydroxide (13 mL) in distilled water (37 mL) was heated to 80° under constant stirring. The substrate containing the polymerized PhC was immersed into the hot Cd precursor solution for 10 minutes to complex the Cd ions on the APTES amino- terminations. A water solution (20 mL) containing thiourea (0.13 g) was then added. The deposition of a 20nm thick CdS layer was observed after 2 minutes. The sample was then extracted and quickly rinsed with excess of fresh distilled water. The linear optical characterization of the CdSs layers has been performed using a UV-1601 Shimazdu bench spectrophotometer. The optical characteristics of the PhC have been measured using a Thermo-Nicolet FTIR microscope in transmission mode pointing the beam in the woodpile stacking direction [44].

3. Results and discussion

Figure 1(a) shows an SEM image of a 60 × 60 × 13.5 μm^3 woodpile structure obtained using commercial Ormocer® resist. The structure is a replica of the template used for CdS deposition [23].

A 10μm thick frame was fabricated around the woodpile arrangement to prevent the structure from collapsing and to minimize the effect of the polymer shrinking during the post-development stage. The in-scale schematic in Fig. 1(b) evidences the spatial repetition of the perpendicular rods.

The lattice period a and the repeated layers height d are related according to $d/a = \sqrt{2}$, which gives the structure a face-centered-cubic (f.c.c.) space group [7]. The rods' surface of the woodpile has then been functionalized with aminopropyl triethoxysilane (APTES) molecules using the residual Ormocer® surface silanols [24] as anchoring sites. A thin layer of Cadmium Sulfide (CdS) has been deposited on the pre-functionalized surface of the PhC using a CBD approach. The APTES amino- terminations coordinate the CdS growth on the woodpile surface complexing the metal ions in solution. No CdS deposition has been observed without the APTES pre-functionalization step.

CdS has been the material of choice in the production of 3D PhCs mainly for inverse opal structures [25–27] since it appealingly combines some of the fundamental materials requirements in photonics: a high refractive index, a marked optical non-linearity and transparency in the visible and near-infra red (NIR) wavelengths region [28,29]. Other binary

#119435 - $15.00 USD Received 3 Nov 2009; revised 17 Dec 2009; accepted 18 Dec 2009; published 7 Jan 2010

bulk chalcogenides (i.e. CdSe) have been deposited for the realization of electro-deposited 2D [30,31] and inverse opals 3D phonic arrays [26]. With the exception of CdS in the form of luminescent quantum dots [32], to the best of the authors' knowledge there is no report in literature of 3D TPP woodpile structures realized using CdS in its bulk form.

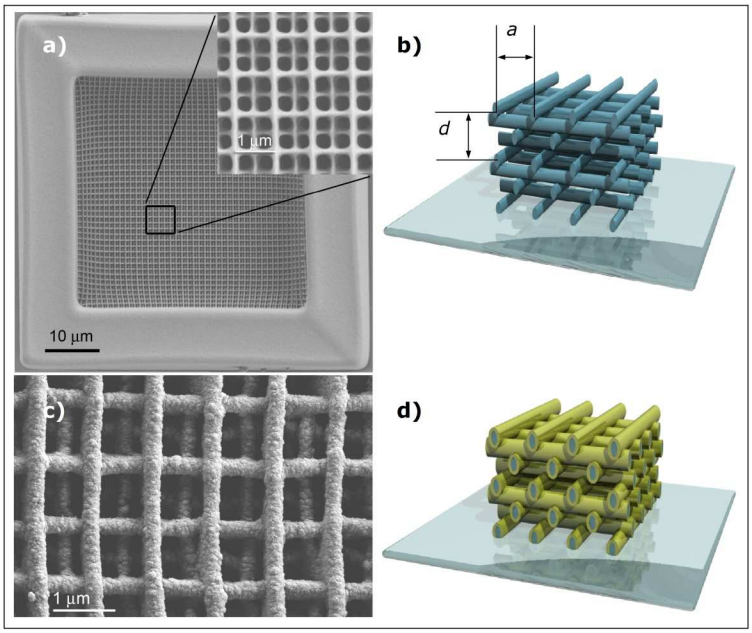

Fig. 1. a) SEM image of the 60x60 µm^2 Ormocer® woodpile structure fabricated using a TPP approach. The schematic in b) shows that the rod spacing *a* and the inter-layer spacing *d* are designed according to an f.c.c. space group ($d/a = \sqrt{2}$). The SEM image in c) shows a particular of the woodpile structure coated with CdS after deposition of an 80 nm layer. Schematic in d) is an in-scale reconstruction of the final CdS coated woodpile.

The APTES-PhC was immersed in the aqueous bath, and the deposition parameters have been adjusted to obtain heterogeneous nucleation of CdS on the functionalized Ormocer® surface, which was found to trigger the growth of continuous semiconductor layers. Undesired homogeneous nucleation of CdS nanocrystals in the solution bulk is avoided by reducing the concentration of free Cd^{2+} ions available for CdS precipitation. Such control is obtained using ammonia as a complexing agent. Only a small concentration of free Cd^{2+} ions is released for CdS formation thanks to the low equilibrium constant of the ammonia-cadmium complex dissociation ($K_e = 10^{-74}$ [33]). In addition, the low solubility product of CdS in the aqueous medium favors heterogeneous chalcogenide formation on the functionalized Ormocer® surface.

The SEM image in Fig. 1(c) shows a portion of the PhC after 4 repetitions of the deposition protocol, while Fig. 1(d) is an in-scale representation of the final coated woodpile. The SEM image demonstrates that the deposited material is homogeneously coating the perpendicular arrangement of the PhC rods. It also reveals the presence of the coating up to 4 vertical repetitions of the PhC rod layers, demonstrating the in-depth penetration of the CBD solution into the PhC structure.To confirm the nature of the coating material, together with its optical and morphological characteristics, the deposition protocol has been performed on flat glass substrates, which were pre-functionalized with an APTES monolayer according to a methodology reported elsewhere [34].

The deposited homogeneous CdS layers appear optically transparent and show a sharp reflectivity. Plots in Fig. 2(a) show the evolution of the transmittance spectra of the film

#119435 - $15.00 USD Received 3 Nov 2009; revised 17 Dec 2009; accepted 18 Dec 2009; published 7 Jan 2010

during multiple-layer deposition. The spectra were taken after each of four sequential depositions (20 minutes each), each one performed using a fresh mother-batch solution.

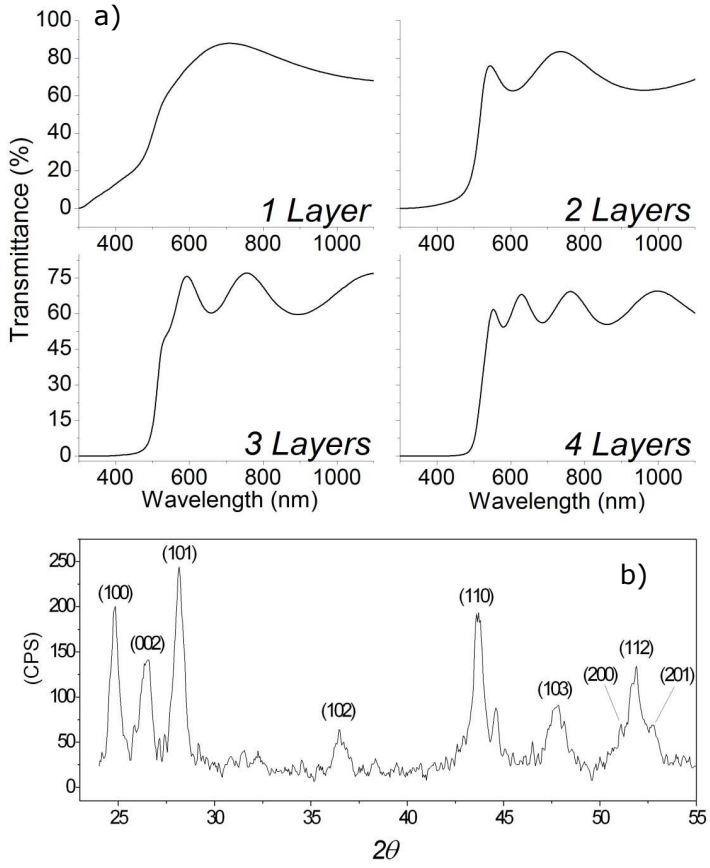

Fig. 2. a) Optical transmittance of CdS films in the 300-1100 nm wavelength range during the sequential deposition of 4 semiconductor layers. Each layer is 200 nm thick. b) X-ray diffraction pattern of an 800 nm thick CdS multilayer showing reflections of CdS hexagonal lattice arrangement.

The measured band-gap at 494nm (2.51eV) is the expected one for bulk CdS [35], while the interference fringes at lower energies indicates the formation of a high-*n* layer. The fringes frequencies allowed for the determination of the layers thickness and refractive index by means of a modified envelope method [36,37]. Each layer was calculated to be about 200nm thick, resulting in a 10nm/min deposition rate.

The layers have a calculated *n* of 2.15 @ 1100nm, in agreement with literature values for CBD of CdS films [35,38]. The layered micro-structure was determined with glancing angle X-Ray Diffraction (XRD), and the resulting diffractogram is shown in Fig. 2(b). The reflection signals are those of crystalline CdS in its hexagonal lattice arrangement, consistent with previously reported data for CBD CdS films [33,39].

The coating protocol adopted for the Ormocer® PhC was four sequential deposition cycles of 2 minutes, leading to an average of one 20nm-thick layer per deposition. Direct measurement of the rod thickness taken from the SEM image of Fig. 1(c) confirms the 20nm deposition layers. The optical characteristics of the CdS coated PhC have been studied with a Fourier-Transform Infra-Red (FTIR) spectroscope measuring the optical transmission of the woodpile along its stacking direction.

#119435 - $15.00 USD Received 3 Nov 2009; revised 17 Dec 2009; accepted 18 Dec 2009; published 7 Jan 2010

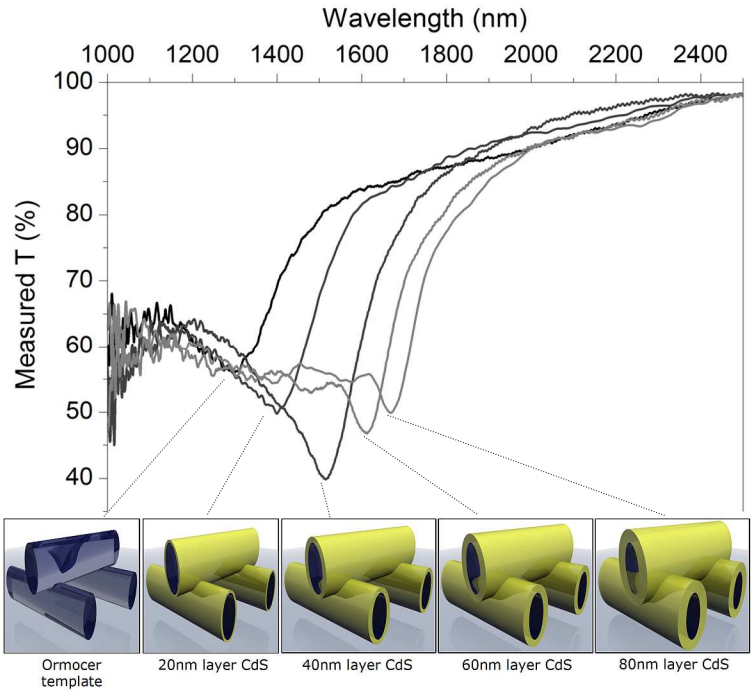

Fig. 3. Measured transmission spectra of the PhC during successive CdS depositions. The raw spectra were collected using the substrate as the reference. The PBG shifts according to the increasing CdS layer thickness on the structure rod surface in the 0–80mn range.

The plots of Fig. 3 reveal the dramatic effect of the CdS layers on the PhC photonic stop band. The initial APTES-functionalized PhC stop band, centered at 1300nm, undergoes a 375nm shift after four CdS layers are deposited. An average PBG shift of more than 90nm is recorded after each one of the four CdS depositions. The PBG shift is remarkably accompanied by a variation of the stop band amplitude, which shows a 17% increase after the deposition of a 40nm CdS layer.

While the PBG shift is related to a combination of geometric (change in rod thickness [24]) and optical effects (increase of the effective refractive index, n_{eff} [23]), the enhanced PBG amplitude is a consequence of the sole n_{eff} increase. A decrease in this tendency is evidenced for CdS layers thicker than 40nm. This trend is attributed to the interplay of the surface roughness of the deposited CdS layers together with a natural decrease of the PBG strength when the optimum filling factor of a woodpile is exceeded [47]. The role of the CdS surface scattering is further highlighted by the appearance of distinguished sub-band transmission in the blue edge of the PBG.

To better expose the combined effect of rod thickness and n_{eff} on the PBG, the band diagram of the woodpile structure before and after each deposition was simulated using the open source MPB software package [40]. The simulation inputs were the geometrical parameters measured from SEM images (Fig. 1) together with the films thickness and the refractive index calculated using the modified envelope method.

The woodpile rod geometry after each CdS deposition was assumed to be that of the starting Ormocer template (144 × 342 nm^2 elliptic sections), increased by a 20nm CdS layer for each one of the deposited layers. The n_{eff} value was calculated by volume averaging the refractive index of the Ormocer template (1.47 [41,42]) and the CdS (2.15 from envelope method). Such volume average was calculated assuming that the intersected rods junctions are not accessible and therefore not coated by the CdS layers.

#119435 - $15.00 USD Received 3 Nov 2009; revised 17 Dec 2009; accepted 18 Dec 2009; published 7 Jan 2010

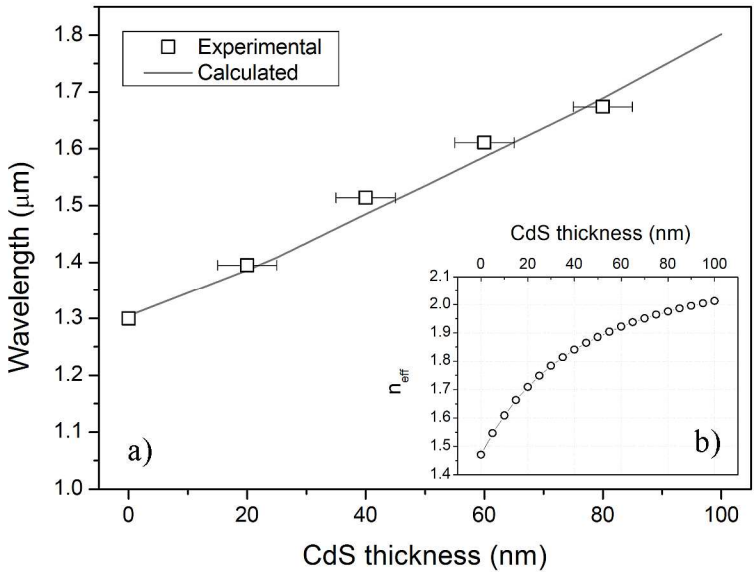

Fig. 4. a) Simulated position of the woodpile PBG (solid line) compared with the measured experimental values (squares) as a function of CdS layer thickness. b) Predicted evolution of n_{eff} with CdS layer thickness on the Ormocer® woodpile rods.

The measured shift of the PBG of the woodpile PhC for each deposition step can be accurately modeled (Fig. 4(a)). The predicted n_{eff} values in Fig. 4(b) illustrate that the method of multi-layer deposition can be used to engineer the refractive index of 3D Ormocer® PhCs; an 80nm chalcogenide layer is shown to increase the woodpile refractive index by 34%. The simulation confirms within a small error (< 5%) the refractive index and thickness values calculated with the envelope method. This in turn validates the robustness of the proposed protocol and underlines its intrinsic accuracy despite its practical simplicity. The optical properties of the entire 3D woodpile PhC can be tuned varying a few experimental parameters, such as precursors' concentration, deposition temperature, and deposition time.

4. Conclusions

In summary, an effective method to tune the refractive index of Ormocer® PhCs obtained with a TPP technique is described. The protocol combines the fabrication flexibility offered by a TPP approach with the favorable optical characteristics of CdS as the binary chalcogenide for photonic applications. The ability to control the CdS deposition parameters, critical to the final optical quality and refractive characteristics of the PhC, makes this method suitable for production of high precision devices. A fine tuning of the PBG wavelength of the PhC over a 375 nm range has been demonstrated, as well as a 17% increase of the PBG amplitude after the deposition of a 40nm CdS layer. With this method it could possible to realize high-*n* and non-linear woodpile PhCs operating in the telecommunication wavelengths or even in the visible wavelengths by modifying the periodicities of the structures.

Acknowledgements

This work was produced with the assistance of the Australian Research Council under the ARC Centers of Excellence program. The authors acknowledge the ARC Centre of Excellence CUDOS (Centre for Ultrahigh-bandwidth Devices for Optical Systems) for the support. Dario Buso acknowledges the ARC for the support through the APD grant DP0988106.

#119435 - $15.00 USD Received 3 Nov 2009; revised 17 Dec 2009; accepted 18 Dec 2009; published 7 Jan 2010